Hindawi
Mathematical Problems in Engineering
Volume 2018, Article ID 3106329, 9 pages
https://doi.org/10.1155/2018/3106329

*Research Article*

# Vehicle Running State Estimation by Adaptive Soft-Sensing Algorithm

**Liang Hao**,[1,2] **Lixin Guo**,[2] **and Shuwei Liu**[1,2]

[1]*Automobile & Traffic Engineering College, Liaoning University of Technology, Jinzhou, Liaoning 121000, China*
[2]*School of Mechanical Engineering & Automation, Automotive Engineering, Northeastern University, Shenyang 110819, China*

Correspondence should be addressed to Liang Hao; hl867438249@126.com

Received 30 August 2018; Accepted 17 October 2018; Published 8 November 2018

Academic Editor: Salvatore Strano



Vehicle running state adaptive unscented Kalman filter soft-sensing algorithm is put forward in this paper based on traditional UKF which can estimate vehicle running state parameters and suboptimal Sage-Husa noise estimator which can effectively solve the problem of noises varying with time. Meanwhile 3-DOF dynamic model of vehicle and HSRI tire model are established. So vehicle running state can be accurately estimated by fusing the low-cost measurement information of longitudinal and lateral acceleration and handwheel steering angle. Under the typical working condition, AUKF soft-sensing algorithm is verified with substantial vehicle tests. Comparing with UKF soft-sensing algorithm, the result indicates AUKF soft-sensing algorithm has a good performance in robustness and is able to realize the effective estimation of vehicle running state more precisely than UKF soft-sensing algorithm.

## 1. Introduction

In recent years, more and more active safety system is matched in the vehicle, but active safety system can well achieve active safety control by the real-time obtaining vehicle running state information. However, as some of their parameters like side slip angle are hard to be measured and have quite a high cost of measurement, it is of vital importance to find out a low-cost method for getting the high-accuracy parameters of distributive vehicles in quite real time.

At present, soft-sensing technology has been widely applied to the estimation of vehicles' dynamic and kinematic parameters. For example, UKF was used to estimate the running state and parameters of vehicles [1, 2]; vehicles' driving state was efficiently estimated by multirate EKF soft-sensing algorithm [3]; what is more, vehicles' state and parameters, respectively, can be estimated by double EKF working at the same time [4, 5]; UKF estimation algorithm was put forward to study the lateral and longitudinal speed of vehicles [6]; UKF was used to estimate vehicle state and road parameters [7, 8].

High-accuracy noise statistical characteristics are required for UKF soft-sensing technology, but noise statistical characteristics are actually varying with time in practice, which is easy to make the estimation accuracy greatly reduced, or even divergent. For that reason, self-adaptive UKF algorithm based on Sage-Husa is established in this paper to avoid the deficiency described above. Meanwhile, multisensor fusion technology is adopted to realize the precise estimation of longitudinal and lateral speed, side slip angle, and yaw rate of electric vehicles. Finally, the validity of the algorithm is verified through the real vehicle test.

## 2. Dynamic Model

*2.1. Vehicle 3-DOF Model.* The model includes longitudinal and lateral speed and yaw rate. In Figure 1, the ISO coordinate system is through the mass center of a vehicle, where the right part of x-axis means the positive and the symmetry axis for longitudinal direction, and the upper part of y-axis means the positive and going through the mass center O.

The dynamic equation derived from the 3-DOF vehicle dynamic model is shown as formula (1):

$$\dot{u} = a_x + v \cdot \gamma$$

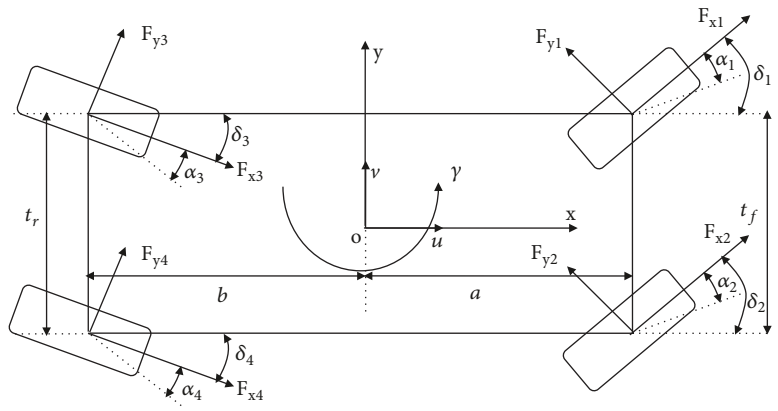


Figure 1: Vehicle 3-DOF dynamic model.

$$
\begin{aligned}
&\dot{v} = a_y - u \cdot \gamma \\
&\dot{\gamma} = \frac{\Gamma}{I_Z} \\
&\Gamma = a\left(F_{x1}\sin\delta_1 + F_{y1}\cos\delta_1\right) - \frac{t_f}{2}\left(F_{x1}\cos\delta_1\right. \\
&\quad \left. - F_{y1}\sin\delta_1\right) + a\left(F_{x2}\sin\delta_2 + F_{y2}\cos\delta_2\right) \\
&\quad + \frac{t_f}{2}\left(F_{x2}\cos\delta_2 - F_{y2}\sin\delta_2\right) - b\left(F_{x3}\sin\delta_3\right. \\
&\quad \left. + F_{y3}\cos\delta_3\right) - \frac{t_r}{2}\left(F_{x3}\cos\delta_3 - F_{y3}\sin\delta_3\right) \\
&\quad - b\left(F_{x4}\sin\delta_4 + F_{y4}\cos\delta_4\right) + \frac{t_r}{2}\left(F_{x4}\cos\delta_4\right. \\
&\quad \left. - F_{y4}\sin\delta_4\right) \\
&\beta = \frac{v}{u} \\
&a_x = \frac{1}{m}\left(F_{x1}\cos\delta_1 - F_{y1}\sin\delta_1 + F_{x2}\cos\delta_2\right. \\
&\quad - F_{y2}\sin\delta_2 + F_{x3}\cos\delta_3 - F_{y3}\sin\delta_3 + F_{x4}\cos\delta_4 \\
&\quad \left. - F_{y4}\sin\delta_4 - F_w\right) \\
&a_y = \frac{1}{m}\left(F_{x1}\sin\delta_1 + F_{y1}\cos\delta_1 + F_{x2}\sin\delta_2\right. \\
&\quad + F_{x2}\cos\delta_2 + F_{x3}\sin\delta_3 + F_{y3}\cos\delta_3 + F_{x4}\sin\delta_4 \\
&\quad \left. + F_{y4}\cos\delta_4\right)
\end{aligned}
\tag{1}
$$

where $u$ is longitudinal speed; $v$ is lateral speed; $\gamma$ is yaw rate; $a_x$ is longitudinal acceleration; $a_y$ is lateral acceleration; $\Gamma$ is torque around z axis; $a$, $b$ denote the distance from mass center to front axis and to back axis; $I_z$ is car inertia around z-axis; $\delta_i$ is wheel steering angle; $i$=1(front left), 2(front right), 3(rear left), 4(rear right); $F_{xj}$ is longitudinal force; $F_{yj}$ is lateral force; $j$=1(front left), 2(front right), 3(left rear), 4(right rear); $F_w$ is wind resistance.

*2.2. HSRI Tire Model.* HSRI is a semiempirical tire model acquired through a number of tire tests carried out by Highway Safety Research Institute of University of Michigan in America. In this paper, a relative simple model form is used because of its simple form and less parameters for identification [9]. Meanwhile, higher accuracy can be achieved without taking the aligning torque of tire into consideration.

For the wheels of vehicle, the longitudinal and lateral force on each tire can be expressed by the following formulas:

$$
F_x = \begin{cases} -C_s\dfrac{S_x}{1-S_x} & \lambda \geq 1 \\ -C_s\dfrac{S_x}{1-S_x}\lambda\left(2-\lambda\right) & 0 < \lambda < 1 \\ -C_s\mu F_z\dfrac{1}{\sqrt{C_s^2 + \left(C_\alpha S_y\right)^2}} & \lambda = 0 \end{cases} \tag{2}
$$

$$
F_y = \begin{cases} -C_\alpha\dfrac{S_y}{1-S_x} & \lambda \geq 1 \\ -C_\alpha\dfrac{S_y}{1-S_x}\lambda\left(2-\lambda\right) & 0 < \lambda < 1 \\ -C_s S_y\mu F_z\dfrac{1}{\sqrt{C_s^2 + \left(C_\alpha S_y\right)^2}} & \lambda = 0 \end{cases} \tag{3}
$$

where $\lambda = \mu F_z(1 - S_x)/2\sqrt{(C_s S_x)^2 + (C_\alpha S_y)^2}$; $\lambda$ is limit of adhesion region; $C_s$, $C_\alpha$ denote longitudinal and lateral slip stiffness; $\mu$ is road friction coefficient; $S_x, S_y$ denote longitudinal and lateral slip rate; $F_z$ is tire vertical force.

The longitudinal slip rate and lateral slip rate on each tire can be expressed by the following formulas:

$$
S_{xij} = \begin{cases} \dfrac{R\omega_{ij} - u_{xij}}{u_{xij}} = \dfrac{R\omega_{ij}}{u_{xij}} - 1 < 0 & u_{xij} \neq 0 \text{ for braking} \\ \dfrac{R\omega_{ij} - u_{xij}}{R\omega_{ij}} = 1 - \dfrac{u_{xij}}{R\omega_{ij}} > 0 & \omega_{ij} \neq 0 \text{ for driving} \end{cases} \tag{4}
$$

$$S_{yij} = \frac{v_{yij}}{u_{xij}} \tag{5}$$

where $\omega_{ij}$ is angular speed of four wheels, $ij$=$fl$ (front left), $fr$ (front right), $rl$ (rear left), $rr$ (rear right); $u_{xij}$, $v_{xij}$ are longitudinal and lateral wheel velocities.

Vertical force can be calculated by

$$\begin{aligned}
F_{z1} &= \left(\frac{1}{2}mg - ma_y\frac{h_g}{t_f}\right)\frac{b}{a+b} - \frac{1}{2}ma_x\frac{h_g}{a+b} \\
F_{z2} &= \left(\frac{1}{2}mg + ma_y\frac{h_g}{t_f}\right)\frac{b}{a+b} - \frac{1}{2}ma_x\frac{h_g}{a+b} \\
F_{z3} &= \left(\frac{1}{2}mg - ma_y\frac{h_g}{t_f}\right)\frac{a}{a+b} + \frac{1}{2}ma_x\frac{h_g}{a+b} \\
F_{z4} &= \left(\frac{1}{2}mg + ma_y\frac{h_g}{t_f}\right)\frac{a}{a+b} + \frac{1}{2}ma_x\frac{h_g}{a+b}
\end{aligned} \tag{6}$$

where $F_{zp}$ is tire vertical force, $p$=1(front left), 2(front right), 3(rear left), 4(rear right); $m$ is car mass; $g$ is gravitational constant; $h_g$ is vehicle height of center of gravity; $a$, $b$ are distance of front and rear wheels from center of gravity; $t_f, t_r$ are distance of the vehicle front and rear longitudinal axis from wheels; $a_x, a_y$ are longitudinal and lateral acceleration.

The longitudinal and lateral wheel velocities can be expressed by the following formulas:

$$\begin{aligned}
u_{xfl} &= \left(u - \gamma\frac{t_f}{2}\right)\cos\delta_1 + (v + \gamma a)\sin\delta_1 \\
v_{yfl} &= -\left(u - \gamma\frac{t_f}{2}\right)\sin\delta_1 + (v + \gamma a)\cos\delta_1 \\
u_{xfr} &= \left(u + \gamma\frac{t_f}{2}\right)\cos\delta_2 + (v + \gamma a)\sin\delta_2 \\
v_{yfr} &= -\left(u + \gamma\frac{t_f}{2}\right)\sin\delta_2 + (v + \gamma a)\cos\delta_2 \\
u_{xrl} &= \left(u - \gamma\frac{t_r}{2}\right)\cos\delta_3 + (v - \gamma b)\sin\delta_3 \\
v_{yrl} &= -\left(u - \gamma\frac{t_r}{2}\right)\sin\delta_3 + (v - \gamma b)\cos\delta_3 \\
u_{xrr} &= \left(u + \gamma\frac{t_r}{2}\right)\cos\delta_4 + (v - \gamma b)\sin\delta_4 \\
v_{yrr} &= -\left(u + \omega\frac{t_r}{2}\right)\sin\delta_4 + (v - \omega b)\cos\delta_4
\end{aligned} \tag{7}$$

## 3. AUKF Soft-Sensing Technology

Soft-sensing technology includes state estimation, neural network, fuzzy mathematics, mechanism modeling, and so on other relative analyzing techniques. It mainly uses those process parameters which can be easily measured to estimate the parameters which cannot be effectively measured, so as to effectively overcome deficiencies on the high cost of hardware measurement or its undetectability in literature [10]. Soft-sensing technology is established based on UKF in this paper.

Instead of traditionally making nonlinear functions linearized, UKF retains the framework of Kalman filter and uses the way of UT to solve the problem of the nonlinear estimation of mean value and covariance in literature [11, 12]. As for the state parameters of a nonlinear system, the estimation made by UKF which keeps higher order terms is more precise and more stable than EKF estimation. However, they both require the quite precise mathematical model of coefficients and noise statistic characteristics. Otherwise, it will lead to reduced estimation accuracy and filtering accuracy or even a divergent result. Therefore, organically combining UKF and suboptimal Sage-Husa noise estimator, the consequent AUKF soft-sensing algorithm can use the suboptimal Sage-Husa noise estimator to realize the real-time estimation for the mean value and covariance matrix of the process noises in this system while the vehicle state is being estimated.

According to the parameters $a_x, a_y, \delta_i$, and $\omega_{ij}$ measured by the vehicle sensor, the unknown vehicle $u$, $v$, and $\gamma$ parameters are further estimated. Since only discrete signals can be processed on computers, the equation for system state discretization works out according to formula (1) is shown as below:

$$\begin{aligned}
x_{k+1} &= f(x_k, u_k) + \varpi_k = \begin{bmatrix} u \\ v \\ \gamma \\ \Gamma \\ a_x \\ a_y \end{bmatrix}_k \\
&= \begin{bmatrix} u \\ v \\ \gamma \\ 0 \\ 0 \\ 0 \end{bmatrix}_k + \begin{bmatrix} a_x + v\gamma \\ a_y - u\gamma \\ \dfrac{\Gamma}{I_z} \\ 0 \\ 0 \\ 0 \end{bmatrix}_k * T + \begin{bmatrix} 0 \\ 0 \\ 0 \\ \Gamma \\ a_x \\ a_y \end{bmatrix}_k + \varpi_k
\end{aligned} \tag{8}$$

Discretization form for system observation equation is

$$\begin{aligned}
z_k &= h(x_k, u_k) + v_k = \begin{bmatrix} a_x \\ a_y \\ \gamma \end{bmatrix}_k \\
&= \begin{bmatrix} 0 & 0 & 0 & 0 & 1 & 0 \\ 0 & 0 & 0 & 0 & 0 & 1 \\ 0 & 0 & 1 & 0 & 0 & 0 \end{bmatrix} \begin{bmatrix} u \\ v \\ \gamma \\ \Gamma \\ a_x \\ a_y \end{bmatrix}_k + v_k
\end{aligned} \tag{9}$$

where state variable $X = [u, v, \omega, T, a_x, a_y]^T$; observed quantity $Z = [a_x \;\; a_y \;\; \gamma]^T$; control variable $u = [\delta_i]$.

$\varpi_k$ and $\upsilon_k$ should be mutually independent white noises. The statistic characteristics of noises are

$$\begin{aligned} E[\varpi_k] &= q_k \\ E[\upsilon_k] &= r_k \\ E\left\{[\varpi_k - q_k][\varpi_i - q_k]^T\right\} &= Q_k \vartheta_{ki} \\ E\left\{[\upsilon_k - r_k][\upsilon_i - r_k]^T\right\} &= R_k \vartheta_{ki} \end{aligned} \tag{10}$$

The vehicle state variables are 6D random variables and their initial mean values $\overline{X} = E(X_0)$ and $P_0 = E[(X_0 - \overline{X})(X_0 - \overline{X})^T]$. By formulae (11) and (12), 13 Sigma points $X$ and relevant weights $\chi$ can be acquired through UT.

①Calculate the 13 Sigma sampling points:

$$\begin{aligned} X^{(0)} &= \overline{X} \quad i = 0 \\ X^{(i)} &= \overline{X} + \left(\sqrt{(6+\lambda)P}\right)_i \quad i = 1 \sim 6 \\ X^{(i)} &= \overline{X} - \left(\sqrt{(6+\lambda)P}\right)_i \quad i = 7 \sim 12 \end{aligned} \tag{11}$$

②Calculate the relevant weights of these sampling points:

$$\begin{aligned} \chi_m^{(0)} &= \frac{\tau}{n+\tau} \\ \chi_c^{(0)} &= \frac{\tau}{n+\tau} + \left(1 - \alpha^2 + \beta\right) \\ \chi_m^{(i)} &= \chi_c^{(i)} = \frac{\tau}{n+\tau} \quad i = 1 \sim 12 \end{aligned} \tag{12}$$

where the subscripts $m$ and $c$ mean the covariances; $\lambda=\alpha^2(6+\kappa)$-6 is scaling coefficient; $\alpha$ which is generally 0.001 is used to fix the Sigma point set around $\overline{X}$; $\kappa$ is a second-order proportional parameter and $\kappa$=0 here; $\beta \geq 0$ is a nonnegative weight coefficient. Generally $\beta$=2.

③Putting Sigma point set in formula (8), further estimation can be made to get $X^{(i)}(k+1 \mid k) = f(X^{(i)}(k \mid k), u_k) + q_k$ and calculate the covariance matrix of system state variables:

$$\begin{aligned} \hat{X}(k+1 \mid k) &= \sum_{i=0}^{2n} \chi_m^{(i)} X^{(i)}(k+1 \mid k) \\ P(k+1 \mid k) &= \sum_{i=0}^{2n} \chi_c^{(i)} \\ &\quad \cdot \left[\hat{X}(k+1 \mid k) - X^{(i)}(k+1 \mid k)\right] \\ &\quad \cdot \left[\hat{X}(k+1 \mid k) - X^{(i)}(k+1 \mid k)\right]^T + \hat{Q}_k \end{aligned} \tag{13}$$

④The new observed quantity $Z^{(i)}(k+1 \mid k) = h(X^i(k+1 \mid k), u_k) + r_{k+1}$ can be acquired by putting Sigma point set in formula (9), and the mean value and covariance of system estimation is acquired by weighted summation:

$$\begin{aligned} \hat{Z}(k+1 \mid k) &= \sum_{i=0}^{2n} \chi_m^{(i)} Z^i(k+1 \mid k) \\ P_{z_k z_k} &= \sum_{i=0}^{2n} \chi_c^{(i)} \left[Z^{(i)}(k+1 \mid k) - \hat{Z}(k+1 \mid k)\right] \\ &\quad \cdot \left[Z^{(i)}(k+1 \mid k) - \hat{Z}(k+1 \mid k)\right]^T + R \\ P_{x_k z_k} &= \sum_{i=0}^{2n} \chi_c^{(i)} \left[X^{(i)}(k+1 \mid k) - \hat{X}(k+1 \mid k)\right] \\ &\quad \cdot \left[Z^{(i)}(k+1 \mid k) - \hat{Z}(k+1 \mid k)\right]^T \end{aligned} \tag{14}$$

⑤Gain matrix $K(k+1) = P_{x_k z_k} P_{z_k z_k}^{-1}$ by which system state update and covariance update can be calculated by

$$\begin{aligned} \hat{X}(k+1 \mid k+1) &= \hat{X}(k+1 \mid k) \\ &\quad + K(k+1)\left[z_{k+1} - \hat{Z}(k+1 \mid k)\right] \\ P(k+1 \mid k+1) &= P(k+1 \mid k) \\ &\quad - K(k+1) P_{z_k z_k} K^T(k+1) \end{aligned} \tag{15}$$

⑥The update of the characteristics of process noise statistics is

$$\begin{aligned} q_{k+1} &= (1 - d_{k+1}) q_k + d_{k+1}\left[\hat{X}(k+1 \mid k+1) - \sum_{i=0}^{2n} \chi_m^{(i)} X^{(i)}(k+1 \mid k)\right] \\ \hat{Q}_{k+1} &= (1 - d_{k+1}) \hat{Q}_k + d_{k+1}\left\{K(k+1) \overset{\cap}{Z}(k+1 \mid k) \cdot \overset{\cap}{Z}^T(k+1 \mid k) K^T(k+1) + P(k+1 \mid k+1) - P_{x_k z_k}\right\} \\ \overset{\cap}{Z}(k+1 \mid k) &= z_{k+1} - \hat{Z}(k+1 \mid k) \\ d_{k+1} &= \frac{(1-f)}{(1-f^{k+1})} \end{aligned} \tag{16}$$

where $c$ is forgetting factor which values from 0.95 to 0.99.

## 4. Algorithm Verification and Analysis

Handwheel steering angle sensor, biaxial speedometer, gyro inertial navigation system, and 1000 Hz sampling frequency data acquisition instrument are placed in a kind of B car. The parameters of vehicle are partly shown in Table 1 and vehicle experiment data's acquisition and analysis procedure are shown in Figure 2. High-speed double lane change

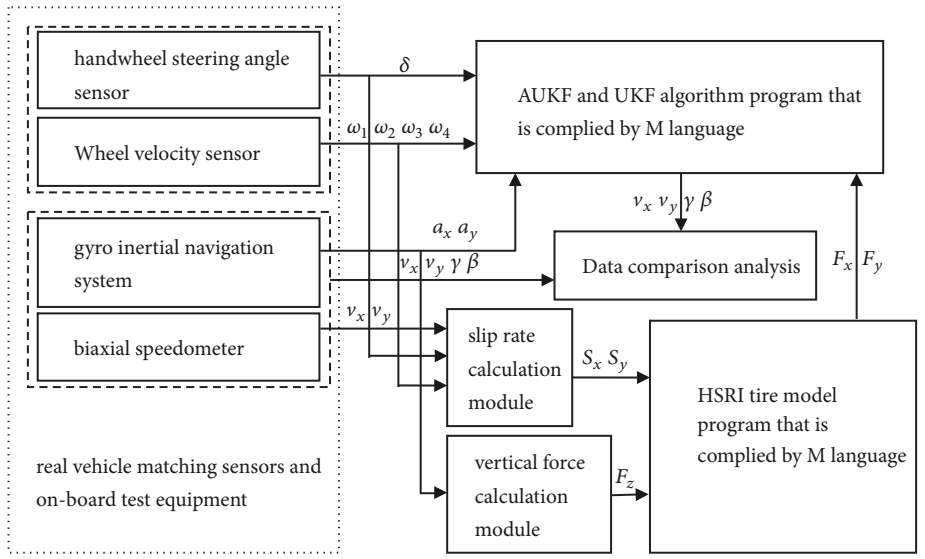


Figure 2: Vehicle test data's acquisition and analysis procedure.

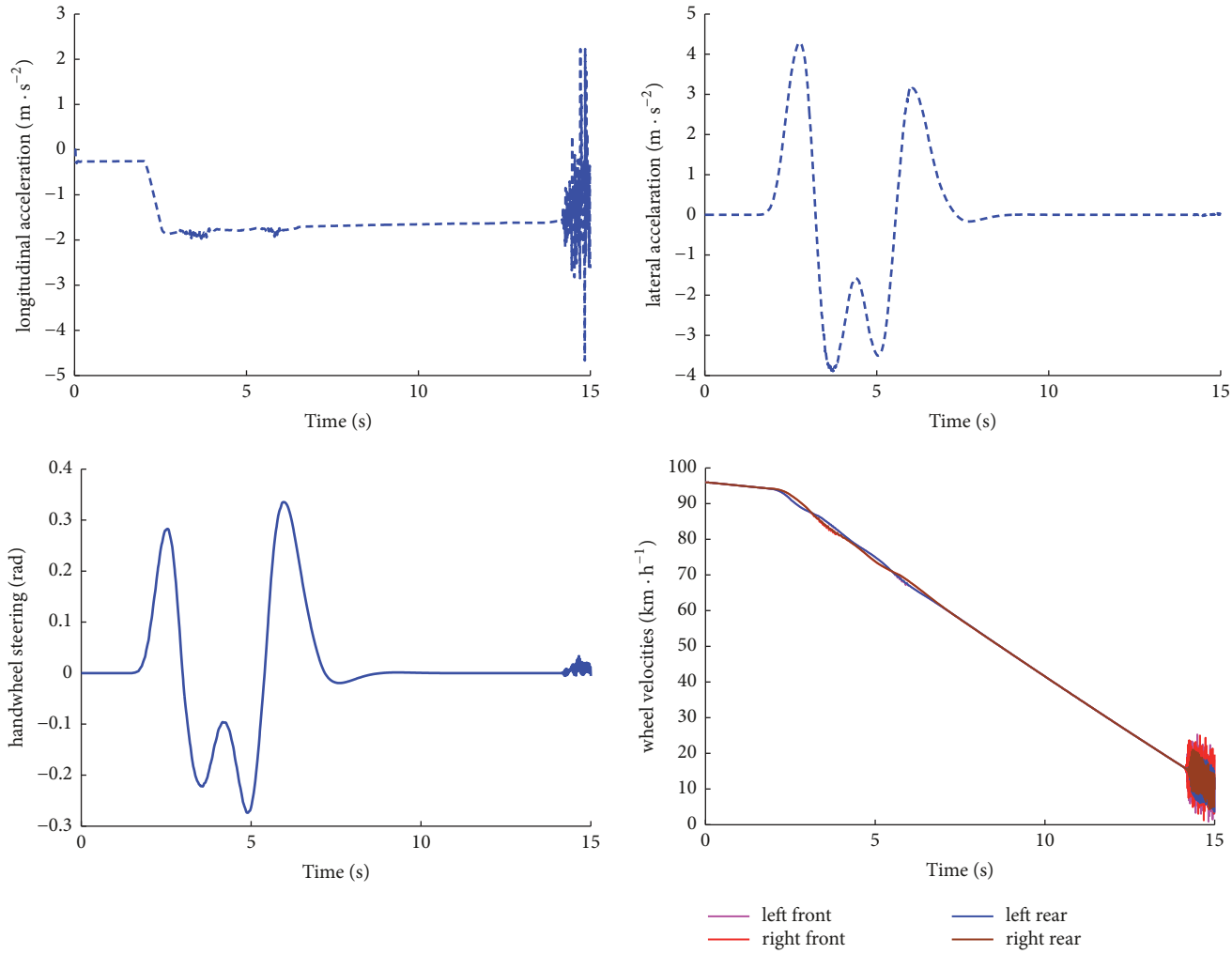


Figure 3: Input signals by the sensors in double lane change emergency braking test.

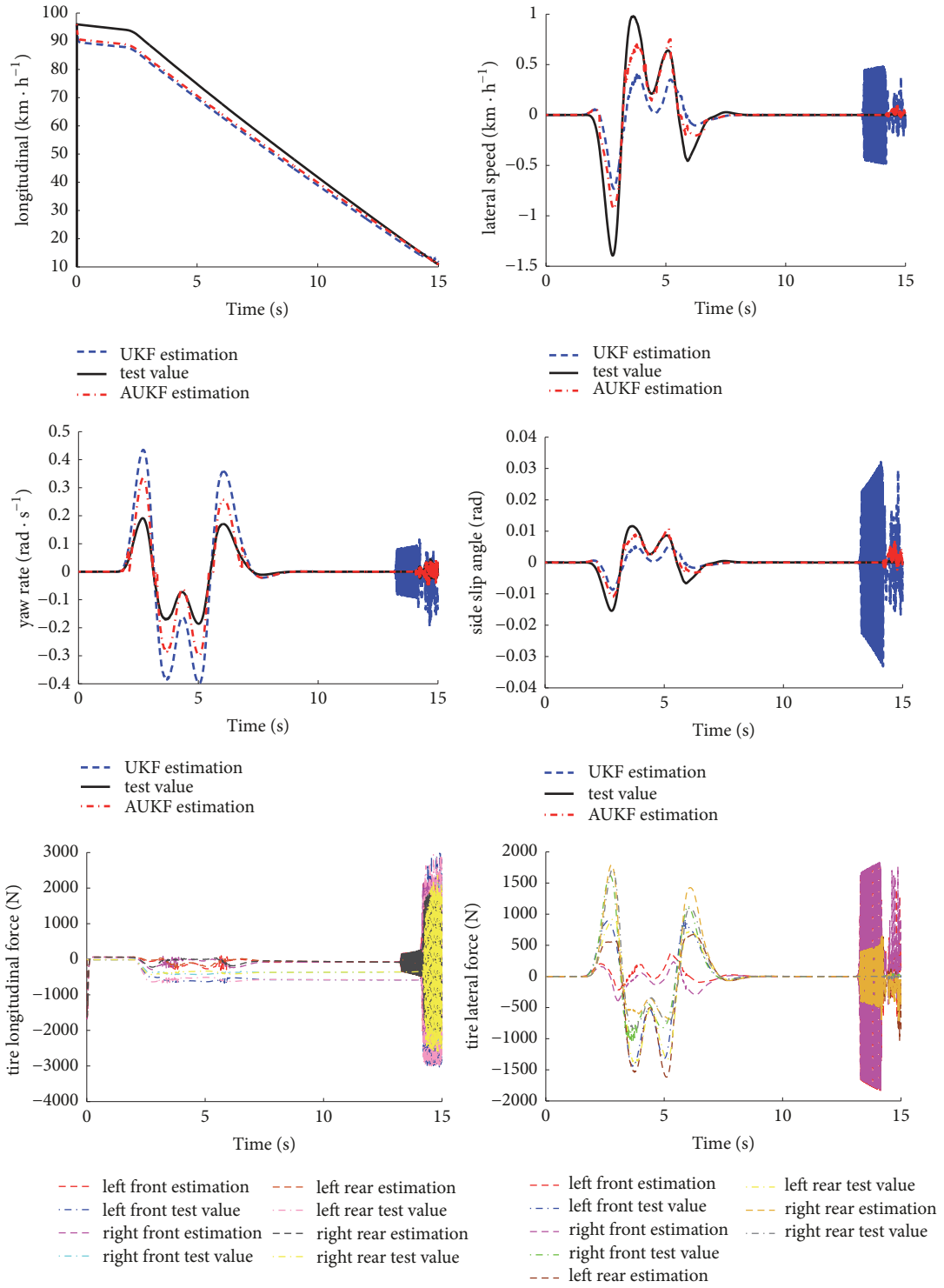


Figure 4: Curves of double lane change emergency braking test.

emergency braking and fishhook emergency braking on dry concrete pavement are chosen to verify AUKF algorithm effectiveness.

*4.1. High-Speed Double Lane Change Braking Test.* According to ISO 3888-1 working condition standard for double lane change test, the initial state value is recorded by biaxial speedometer and gyro inertial navigation system. Road friction coefficient is 0.8 and 0.68 Mpa pressure caused by the brake master cylinder for emergency braking in the second second.

In order that the algorithm can realize the accurate soft measurement of vehicle state, it is critical to properly identify the initial value for AUKF estimation. The initial values are

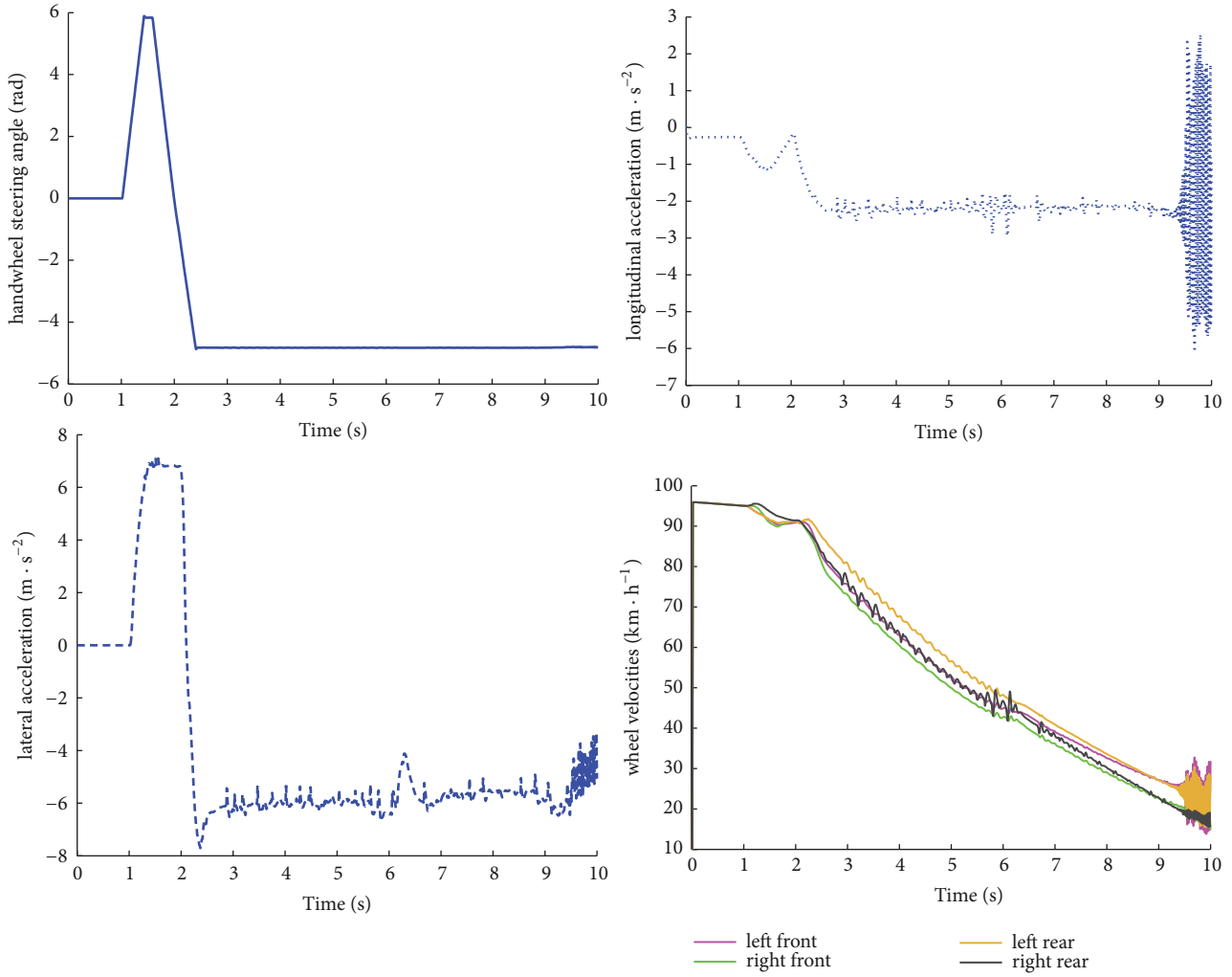


Figure 5: Input signals by the sensors in the fishhook emergency braking test.

Table 1: Vehicle some parameters.

| Parameters | values |
|---|---|
| Car mass $m$/kg | 1170 |
| Distance of front wheels from center of gravity $a$/m | 0.998 |
| Distance of rear wheels from center of gravity $b$/m | 0.998 |
| Distance of front longitudinal axis from wheels $t_f$/m | 1.481 |
| Distance of rear longitudinal axis from wheels $t_r$ /m | 1.481 |
| Height of center of gravity $h_g$/m | 0.54 |
| Wheel radius $R$/m | 0.26 |
| Inertia around x axis $I_x$/kg·m$^2$ | 200 |
| Inertia around y axis $I_y$/kg·m$^2$ | 1200 |
| Inertia around z axis $I_z$/kg·m$^2$ | 1200 |
| Vehicle steering Angle transmission ratio $i$ | 17 |

the covariance matrix of system errors $P = zeros(6, 6)$, the covariance matrix of system excitation noises $Q = eye(6) * 0.00001$, the covariance matrix of measured noises $R = eye(3) * 0.001$, the mean value of process noises $q = zeros(6, 1)$, and the mean value of measured noises $r = zeros(3, 1)$.

Longitudinal and lateral speed, side slip angle, and yaw angle rate are estimated with effect through the efficient information fusion of longitudinal and lateral acceleration, wheel velocities, and the handwheel steering angle (see Figure 3). The test results are shown in Figure 4.

According to the curves of longitudinal speed in Figure 4, it shows that self-adaptive AUKF algorithm does better than UKF algorithm in terms of accuracy, stability, astringency, and real-time performance. According to the curves of lateral speed in Figure 4, it is easy to see that AUKF performs better than UKF on the whole and in astringency. Yaw rate curves show that comparing with UKF in Figure 4. AUKF is clearly more accurate on the whole and has a good performance in stability and astringency. Side slip angle curves show that AUKF has higher accuracy of side slip angle estimation on the whole and better astringency in Figure 4. According to Figure 3, lateral acceleration is less than $|0.4\,g|$ on the whole, so vehicle is in linear motion state that tire lateral force depends linearly on side slip angle. According to Figure 4, the real-time

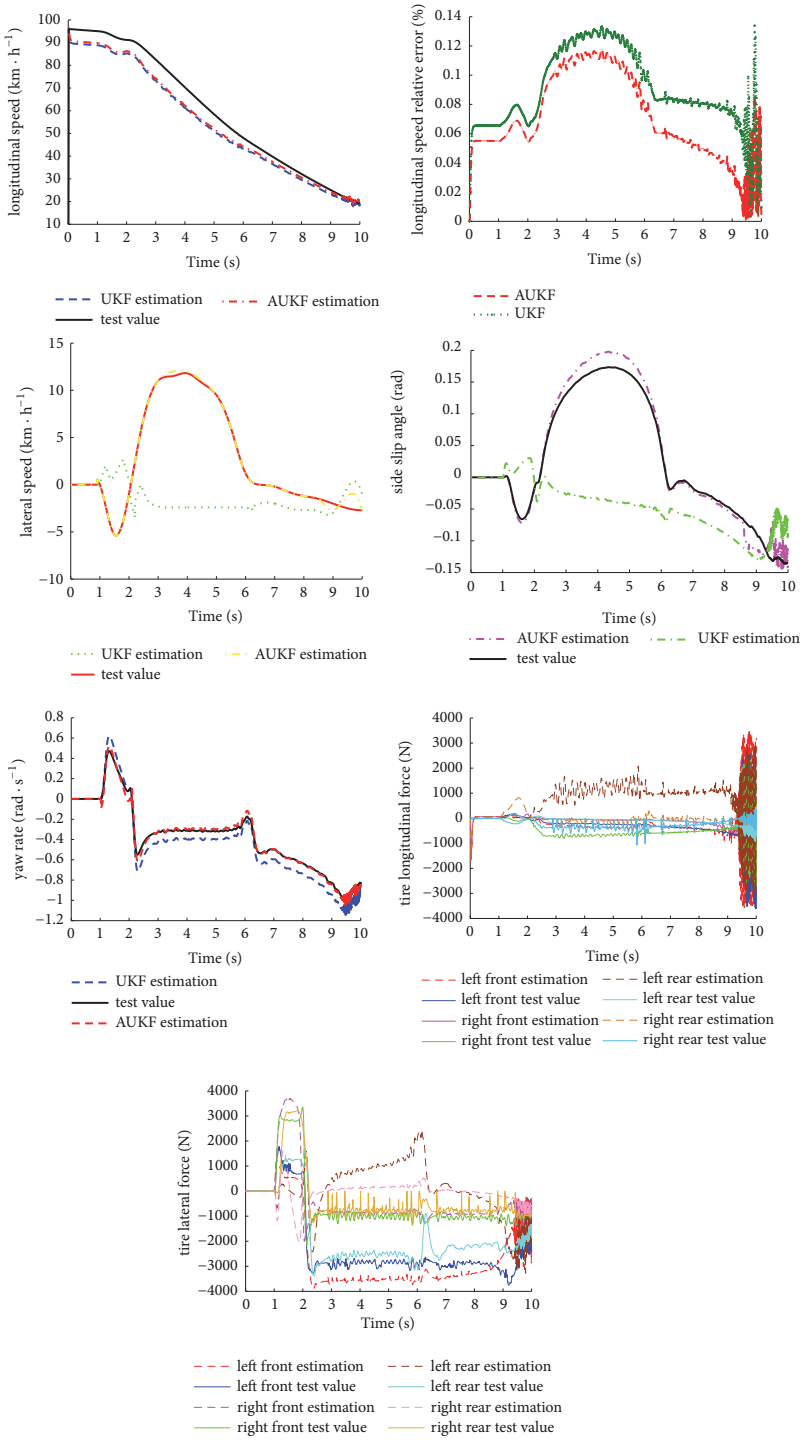


Figure 6: Curves of fishhook emergency braking test.

tire longitudinal and lateral force can be calculated by HSRI tire model, and ultimately the calculated values can well track and converge to the actual values.

*4.2. Fishhook Braking Test.* The initial state value is recorded by biaxial speedometer and gyro inertial navigation system. Road friction coefficient is 0.8 and 0.47 Mpa pressure caused by the brake master cylinder for emergency braking in the second second. The covariance matrix of system errors $P = zeros(6, 6)$, the covariance matrix of system excitation noises $Q = eye(6) * 0.001$, the covariance matrix of measured noises $R = eye(3) * 1000$, the mean value of process noises $q = zeros(6, 1)$, and the mean value of measured noises $r = zeros(3, 1)$.

Longitudinal and lateral speed, side slip angle, and yaw angle rate are estimated with effect through the efficient information fusion of longitudinal and lateral acceleration, wheel velocities, and the handwheel steering angle (see Figure 5). The simulation result is shown in Figure 6.

According to the curves of longitudinal speed and its error, respectively, in Figure 6, they show that self-adaptive AUKF algorithm does better than UKF algorithm in terms of accuracy, stability, astringency, and real-time performance. According to lateral speed curves in Figure 6, AUKF did more better in estimation results, stability, and final astringency than UKF; and the side slip angle features in Figure 6 are the same as the features of the estimated lateral speed. According to yaw rate curves in Figure 6, AUKF performs better than UKF in the general estimation of yaw rate, and the same thing happens in terms of the overall stability and astringency. According to Figure 5, lateral acceleration is greater than $|0.4g|$ in some time area, so vehicle is in nonlinear motion state that tire lateral force depends nonlinearly on side slip angle. According to Figure 6, the real-time tire longitudinal and lateral force can also be calculated when HSRI tire model is in nonlinear motion interval, and ultimately the calculated values well track and converge to the actual values.

## 5. Conclusion

(1) According to the 3-DOF dynamic model, self-adaptive AUKF soft-sensing algorithm was established, integrating the signals of longitudinal and lateral acceleration and handwheel steering angle which were measured by low-cost sensors. In this way, the state parameters of running vehicle, such as longitudinal speed, lateral speed, yaw rate, and side slip angle, can be estimated more accurately even under the premise of vehicle parameters perturbation.

(2) AUKF soft-sensing algorithm was verified using substantial vehicle tests under the premise of the same HSRI tire model that produces the same tire force error. The results have shown that, comparing with UKF, AUKF performed better in accuracy and robustness.

## Data Availability

The data used to support the findings of this study are available from the corresponding author upon request.

## Conflicts of Interest

The authors declare that they have no conflicts of interest.

## Acknowledgments

This work was supported by the National Natural Science Fund Project (50875041), New Century Excellent Talents Support Project (NCET-08-0103), and Major Science and Technology Platform Project of Liaoning Province Education Department (JP2016011).

## References

[1] H. Ren, S. Chen, G. Liu, and K. Zheng, "Vehicle state information estimation with the unscented Kalman filter," *Advances in Mechanical Engineering*, vol. 2014, no. 86, pp. 1120–1146, 2014.

[2] S. Antonov, A. Fehn, and A. Kugi, "Unscented Kalman filter for vehicle state estimation," *Vehicle System Dynamics*, vol. 49, no. 9, pp. 1497–1520, 2011.

[3] R. Anderson and D. M. Bevly, "Using GPS with a model-based estimator to estimate critical vehicle states," *Vehicle System Dynamics*, vol. 48, no. 12, pp. 1413–1438, 2010.

[4] C. Cheng and D. Cebon, "Parameter and state estimation for articulated heavy vehicles," *Vehicle System Dynamics*, vol. 49, no. 1-2, pp. 399–418, 2011.

[5] T. A. Wenzel, K. J. Burnham, M. V. Blundell, and R. A. Williams, "Dual extended Kalman filter for vehicle state and parameter estimation," *Vehicle System Dynamics*, vol. 44, no. 2, pp. 153–171, 2006.

[6] T. Chen, X. Xu, L. Chen, H. Jiang, Y. Cai, and Y. Li, "Estimation of longitudinal force, lateral vehicle speed and yaw rate for four-wheel independent driven electric vehicles," *Mechanical Systems and Signal Processing*, vol. 101, pp. 377–388, 2018.

[7] W. He, N. Williard, C. Chen, and M. Pecht, "State of charge estimation for electric vehicle batteries using unscented kalman filtering," *Microelectronics Reliability*, vol. 53, no. 6, pp. 840–847, 2013.

[8] Y. Xu, B. Chen, and C. Chi, "Estimation of road friction coefficient and vehicle states by 3-DOF dynamic model and HSRI model based on information fusion," *Asian Journal of Control*, vol. 20, no. 3, pp. 1067–1076, 2018.

[9] K. Saadeddin, M. F. Abdel-Hafez, and M. A. Jarrah, "Estimating vehicle state by GPS/IMU fusion with vehicle dynamics," *Journal of Intelligent & Robotic Systems*, vol. 74, no. 1-2, pp. 147–172, 2014.

[10] Te Chen, Long Chen, Xing Xu, Yingfeng Cai, Haobin Jiang, and Xiaoqiang Sun, "Reliable Sideslip Angle Estimation of Four-Wheel Independent Drive Electric Vehicle by Information Iteration and Fusion," *Mathematical Problems in Engineering*, vol. 2018, Article ID 9075372, 14 pages, 2018.

[11] S. Melzi and E. Sabbioni, "On the vehicle sideslip angle estimation through neural networks: numerical and experimental results," *Mechanical Systems and Signal Processing*, vol. 25, no. 6, pp. 2005–2019, 2011.

[12] Bao Han, Guan Xin, Jia Xin, and Liu Fan, "A Study on Maneuvering Obstacle Motion State Estimation for Intelligent Vehicle Using Adaptive Kalman Filter Based on Current Statistical Model," *Mathematical Problems in Engineering*, vol. 2015, Article ID 515787, 14 pages, 2015.